Development 134, 1593-1604 (2007) doi:10.1242/dev.02824

# Independent requirements for Hedgehog signaling by both the anterior heart field and neural crest cells for outflow tract development

**Matthew M. Goddeeris[1], Robert Schwartz[2], John Klingensmith[1] and Erik N. Meyers[1,*]**

Cardiac outflow tract (OFT) septation is crucial to the formation of the aortic and pulmonary arteries. Defects in the formation of the OFT can result in serious congenital heart defects. Two cell populations, the anterior heart field (AHF) and cardiac neural crest cells (CNCCs), are crucial for OFT development and septation. In this study, we use a series of tissue-specific genetic manipulations to define the crucial role of the Hedgehog pathway in these two fields of cells during OFT development. These data indicate that endodermally-produced SHH ligand is crucial for several distinct processes, all of which are required for normal OFT septation. First, SHH is required for CNCCs to survive and populate the OFT cushions. Second, SHH mediates signaling to myocardial cells derived from the AHF to complete septation after cushion formation. Finally, endodermal SHH signaling is required in an autocrine manner for the survival of the pharyngeal endoderm, which probably produces a secondary signal required for AHF survival and for OFT lengthening. Disruption of any of these steps can result in a single OFT phenotype.

**KEY WORDS: Anterior heart field (AHF), Neural crest, Shh, Outflow tract, Congenital heart defect, Hedgehog, Cre, loxP, Septation, Mouse**

## INTRODUCTION

The morphogenesis of the outflow tract (OFT) of the heart is a complex process that is disrupted in the majority of serious congenital heart defects. The OFT begins as an endothelial cell-lined channel surrounded by cardiac muscle. Cells are added to lengthen and to ultimately septate the OFT into the aortic and pulmonary arteries. There are two distinct cell populations that contribute to the OFT after the formation of the initial heart tube – the cardiac neural crest cells (CNCCs) and the anterior heart field (AHF). An important question in heart development is which signaling pathways coordinate the development of CNCCs with the AHF?

Neural crest cells (NCCs) are multi-potential and migrate to populate numerous structures in the embryo. CNCCs are a distinct subpopulation of neural crest originating from the post-otic rhombencephalon to the third somite and migrating into the third, fourth and sixth pharyngeal arches and into the OFT of the heart (Ferguson and Graham, 2004; Hutson and Kirby, 2003; Kirby and Stewart, 1983). CNCCs migrate in close proximity to both the AHF and the pharyngeal endoderm (reviewed in Harvey, 2002). CNCCs are crucial for two separate OFT-related processes: for the control of normal myocardial differentiation, and OFT septation, via population of the OFT endocardial cushions and for the formation of the aorticopulmonary septum (Kirby et al., 1983; Waldo et al., 1999).

The AHF in mouse includes the early pharyngeal core arch mesoderm and splanchnic mesoderm, which overlies the ventral pharyngeal endoderm and can be identified by distinct markers within the primary heart field as early as the cardiac-crescent stage (Cai et al., 2003; Ilagan et al., 2006; Kelly et al., 2001). AHF cells contribute to definitive OFT myocardium as well as to the right ventricle and to some endocardium (Kelly and Buckingham, 2002; Noden, 1991; Verzi et al., 2005; Ward et al., 2005). Previous data have suggested that AHF and CNCCs may be interdependent, because ablation of CNCCs results in changes in OFT length, whereas loss of *Fgf8* can negatively impact both CNCC and AHF development (Hutson and Kirby, 2003; Ilagan et al., 2006; Park et al., 2006; Waldo et al., 1999; Yelbuz et al., 2002).

One signaling pathway that is crucial for heart development is that of Hedgehog (Hh). The Hh ligand sonic hedgehog (*Shh*) is required for OFT development, because $Shh^{-/-}$ mutants have a single OFT. These defects seem to be the result of both CNCC and AHF defects (Washington Smoak et al., 2005). Although *Shh* is not overtly expressed at early stages within the developing heart, it is expressed in the ventral neural tube and ventral pharyngeal endoderm, and could therefore directly affect CNCC and AHF cell development.

Hh signaling from the early endoderm has been implicated as being important in initial myocyte specification. Mouse mutants lacking the obligate Hh receptor smoothened (*Smo*) exhibit downregulated expression of *Nkx2.5*, whereas loss of the inhibitor patched homolog 1 (*Ptch1*) results in the upregulation of this gene (Zhang et al., 2001). Recently, more interest has focused on the role of the pharyngeal endoderm in later heart remodeling events (Brown et al., 2004; Garg et al., 2001; Hu et al., 2004; Ilagan et al., 2006; Xu et al., 2004). The OFT defects observed in $Shh^{-/-}$ mice and the *Shh* expression detected within the pharyngeal endoderm strongly suggest a role for this SHH-signal source in OFT development.

Here, we use conditional gene ablation to generate several tissue-specific Hh pathway mutants to identify the crucial source of SHH and its target tissues during OFT development. These data demonstrate the first known pharyngeal endodermal signal directly required by both the AHF and CNCC fields for OFT morphogenesis, and dissects the relationship between these two fields.

[1]Departments of Cell Biology and Pediatrics, Neonatal-Perinatal Research Institute, Duke University Medical Center, Durham, NC 27710, USA. [2]Baylor College of Medicine, Houston, TX 77030, USA.

*Author for correspondence (e-mail: meyer031@mc.duke.edu)

**Accepted 30 January 2007**

## MATERIALS AND METHODS

### Mouse lines

All mice used in this study were maintained on an outbred genetic background. *Nkx2.5$^{Cre}$* is a *Cre* insert into the *Nkx2.5* locus, rendering it a null allele (Moses et al., 2001). *Shh$^{-/+}$* (*Shh$^{Tm1Chg}$*) is a targeted gene disruption resulting in a null allele (Chiang et al., 1996). The *Shh$^{flox}$* line (*Shh$^{tm2Amc}$* Jax #004293) contains loxP sites surrounding exon 2. This allele maintains wild-type expression prior to recombination (Lewis et al., 2001). The *Smo$^{flox}$* targeted allele (*Smo$^{tm2Amc}$* Jax #004288) contains loxP sites surrounding the first exon (Long et al., 2001; Zhang et al., 2001). A *Smo$^{-}$* (null) allele was generated by crossing the *Smo$^{flox}$* allele to *b-actin-Cre* (gift from M. Lewandoski, NCI, MD), an allele with germline *Cre* expression, and subsequently crossing out the *Cre* allele by backcrossing to ICR (Institute for Cancer Research outbred CD-1, Harlan Sprague Dawley). *Smo$^{OEX}$* [*Gt(ROSA)26Sor$^{tm1(Smo/YFP)Amc}$* Jax #005130] is a targeted allele whereby a constitutively active *Smo-EYFP* fusion gene was inserted into the *Rosa26* locus, expression of which is blocked by a loxP-flanked STOP fragment (Jeong et al., 2004). The *Ptch1$^{lacZ}$* (*Ptch1$^{TmxMS}$* Jax #003081) line is a null allele because the *lacZ* insert replaces exons 1 and 2 (Goodrich et al., 1997). *Mef2C-AHF-Cre*, a transgenic line using *Mef2C* promoter elements, was kindly provided by B. Black (UCSF, CA) (Verzi et al., 2005). *Wnt1-Cre* [*Tg(Wnt1-cre)11Rth* Jax #003829] uses an enhancer of the *Wnt1* gene to express *Cre* in early NCCs (Danielian et al., 1998), whereas *P0-Cre* [*Tg(P0-Cre)1Ky*] expresses *Cre* in migratory NCC precursors and is driven using promoter elements of protein P0 (Yamauchi et al., 1999). The endothelial β-galactosidase marker *Tie2-lacZ* [*Tg(TIE2-lacZ)182Sato/J* Jax #002856] uses an endothelial-cell-specific *Tie2* promoter element (Schlaeger et al., 1997). *TroponinT-Cre* (*TnT-Cre*), a myocardial-specific *Cre*, uses rat *TnT* promoter elements to control the expression of *Cre* and was a gift provided by K. Jiao (University of Alabama at Birmingham, AL). *Tie2-Cre* [*Tg(Tek-cre)12Flv* Jax #004128] expresses *Cre* under the control of the tyrosine kinase *Tek* (Koni et al., 2001). The Cre reporter allele *R26R* [*Gt(Rosa)26Sor$^{tm1Sor}$* Jax #003474) constitutively expresses *lacZ* in cells after Cre recombination (Soriano, 1999). *Fgf8$^{lacZ}$* is a 'knock-in' allele into the *Fgf8* locus (Ilagan et al., 2006). In all figures, wild-type (WT) refers to littermates that are either Cre(+) and flox/+ heterozygous, or flox/flox but Cre(–), unless otherwise specified.

### Generation of Cre-mediated *Shh*- and *Smo*-null mutants

*Nkx2.5$^{Cre/+}$; Shh$^{+/-}$* males were mated with *Shh$^{flox2}$* females to generate *Nkx2.5$^{Cre/+}$; Shh$^{flox/-}$* mutant embryos. Additional alleles (*Ptch1$^{lacZ}$* or *Tie2-lacZ*) were carried by the male in the generation of *Nkx2.5$^{Cre}$* mutants (see Results). Embryos were genotyped for *Cre* (Meyers et al., 1998), and for the presence of the *Shh$^{flox}$* and wild-type alleles (Lewis et al., 2001). *Smo*-null mutant embryos were generated via similar mating schemes, except that *Ptch1$^{lacZ}$* or *Tie2-lacZ* alleles were carried by *Smo$^{flox2}$* females. Embryos were typed for *Cre* and for the *Smo* wild-type allele (Zhang et al., 2001). Embryonic day (E) is defined as E0.5 on day of vaginal plug.

### Dissection, imaging and β-galactosidase staining

Embryos were dissected in either di-ethylpolycarbonate (DEPC)-treated phosphate-buffered saline (PBS) or PBS containing 0.1% Triton X-100 (PBT). Fixation was in 4% paraformaldehyde (PFA) overnight at 4°C. Mutant embryos at E11.5 and earlier were somite-count matched to wild-type littermates. For detection of β-galactosidase activity (β-gal), embryos were fixed for 5 minutes (E9.5) or 10 minutes (E10.5 and older) at room temperature in 2% formaldehyde/0.2% glutaraldehyde in PBS with 0.02% NP40, and were then stained overnight at 37°C in standard X-gal stain or Bluo-Gal stain (5-Bromo-3-Indolyl-β-D-Galactopyranoside, Sigma B2904). Bluo-Gal provides a deeper blue color than the standard stain, allowing for better visualization during section analysis. Control and mutants were treated with the same stain in all cases. Embryos were then either cleared with glycerol or were embedded in paraffin and sectioned using standard procedures (Hogan, 1994).

### In situ hybridization

Whole-mount in situ hybridization with Digoxygenin-labeled antisense riboprobes has previously been described (Neubuser et al., 1997). All riboprobes have been previously reported: *Ap2α* (*Tcfap2a* – Mouse Genome Informatics) (Mitchell et al., 1991), *CrabP1* (Stoner and Gudas, 1989), *Shh* (Echelard et al., 1993), *Tbx1* (Chapman et al., 1996) and *Fgf8* (Crossley and Martin, 1995).

### Immunohistochemistry and cell death analysis

Whole-mount immunohistochemistry was performed as previously described (Washington Smoak et al., 2005). Primary antibodies were used at the following concentrations: 2H3 (1:3 supernatant; Developmental Studies Hybridoma Bank and developed by T. Jessel and J. Dodd, Columbia University, New York, NY), PECAM-1 (1:250; PharMingen, CN557355) and AP2α (1:4; 3B5 supernatant, Developmental Studies Hybridoma Bank and developed by T. Williams, University of Colorado, Denver, CO). Cell proliferation was determined using anti-phosphorylated histone H3 antibody (1:1000; Upstate Biotechnology). Cell death analysis was performed using Lysotracker Red, a lysosomal marker previously shown to indicate cell death (Zucker et al., 1999) as described by Abu-Issa et al. (Abu-Issa et al., 2002). All in situ and immunohistochemistry results are from at least three mutants and three controls.

### Confocal analysis and image handling

Confocal microscopy was performed on a Zeiss LSM 510 META. Images were prepared in Adobe Photoshop 7.0.1. Control and mutant embryos were treated identically and are representative of the data set as a whole.

## RESULTS

### Deletion of *Shh* using *Nkx2.5$^{Cre}$* results in loss of pharyngeal endoderm Hh signaling activity

Complete loss of *Shh* results in multiple developmental abnormalities, including cardiovascular defects such as a single OFT vessel (Washington Smoak et al., 2005). Given the wide range of functions for SHH, it is possible that the cardiovascular defects are due to the abnormal development of the embryo as a whole. Equally plausible is that SHH signaling has a direct function on OFT development. Described signaling sources of SHH that may impact early morphogenesis of the heart include the pharyngeal endoderm, notochord and ventral floorplate (Fig. 1A,C) (Moore-Scott and Manley, 2005). Both the AHF and the CNCCs are in juxtaposition to the pharyngeal endoderm adjacent to the OFT (Harvey, 2002). Additionally, expression of the downstream target *Ptch1* demonstrates high levels of Hh activity in the pharyngeal endoderm and overlying mesenchyme (Fig. 1E,E′).We therefore sought to test the hypothesis that the pharyngeal endodermal domains of *Shh* act directly on the AHF and CNCCs during OFT development.

To test this hypothesis, we genetically ablated *Shh* in the *Nkx2.5$^{Cre}$* domain and compared the resulting phenotypes to those observed in *Shh$^{-/-}$* mutants. *Nkx2.5$^{Cre}$* is expressed throughout the heart tube, pharyngeal endoderm, AHF and first arch ectoderm (Fig. 1B and see Fig. S1 in the supplementary material). The pharyngeal endoderm is the only apparent region of overlap between *Nkx2.5$^{Cre}$* and *Shh* expression (Fig. 1A,B and our unpublished observations). This suggests that *Nkx2.5$^{Cre}$*-mediated deletion results in loss of *Shh* expression specifically within the pharyngeal endoderm.

To confirm that this strategy effectively and specifically ablates pharyngeal endoderm expression of *Shh*, we detected *Shh* mRNA via whole-mount in situ hybridization (Fig. 1C,D). Whereas other expression domains remained intact, we found a specific loss of *Shh* mRNA within the pharyngeal endoderm. Moreover, *Nkx2.5$^{Cre/+}$; Shh$^{flox/-}$; Ptch1$^{lacZ/+}$* triple-mutant embryos exhibited a specific loss of Hh activity, as demonstrated by the absence of *Ptch1$^{lacZ}$* expression in the pharyngeal

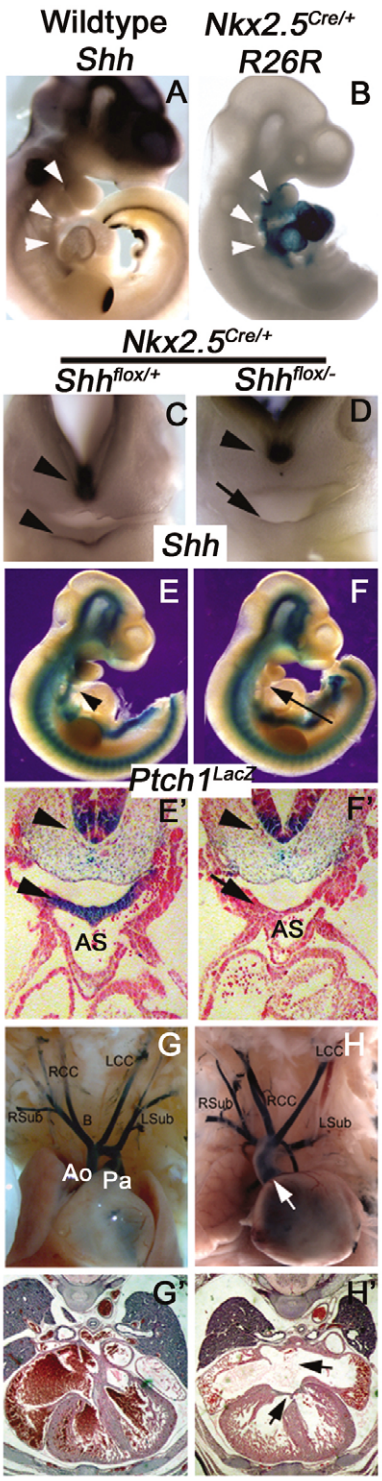


**Fig. 1. *Nkx2.5$^{Cre/+}$; Shh$^{flox/–}$* specifically ablates pharyngeal endodermal SHH and results in a failure of OFT septation.** (**A**) *Shh* is detected by in situ hybridization in the pharyngeal endoderm (arrowheads) at E10.5. (**B**) *Nkx2.5$^{Cre}$* expression, as detected by *R26R*, demonstrates overlap with *Shh* expression in the pharyngeal endoderm alone (arrowheads). (**C**,**D**) Conditional ablation of *Shh* in E10.5 *Nkx2.5$^{Cre/+}$; Shh$^{flox/–}$* embryos results in the specific loss of pharyngeal endodermal *Shh* (arrow, C versus D), but not of notochord and floorplate *Shh* expression, as expected (arrowheads, C,D). (**E-F′**) *Ptch1$^{lacZ}$* expression at E10.5 demonstrates a specific loss of Hh activity in the pharyngeal endoderm and overlying mesoderm and mesenchyme (arrows, F,F′) while maintaining other domains of expression, such as in the floorplate of the neural tube (arrowheads, E-F′). (**G-H′**) Wild-type and *Nkx2.5$^{Cre/+}$; Shh$^{flox/–}$* E18.5 ink injections (G,H) demonstrate a single OFT vessel in mutants (arrow in H), whereas section analysis (G′,H′) reveals a complete atrioventricular canal defect (arrows in H′). In all panels, arrows and arrowheads mark abnormal and normal findings, respectively, in mutants as compared with control embryos. B; brachiocephalic artery; LCC, left common carotid; LSub, left subclavian; OFT, outflow tract; RCC, right common carotid; RSub, right subclavian.

endoderm and arches (Fig. 1E-F′). Combined, these results highlight *Nkx2.5$^{Cre/+}$; Shh$^{flox/–}$* as a possible endodermal-specific deletion of Shh.

## Loss of *Shh* in the pharyngeal endoderm recapitulates cardiac defects observed in *Shh$^{–/–}$* embryos

Similar to *Shh$^{–/–}$* mutants, near-term *Nkx2.5$^{Cre/+}$; Shh$^{flox/–}$* double mutants had single, unseptated OFT vessels (9/10) and reduced right ventricles, leaving their hearts with a small, rounded appearance (Fig. 1G,H). Abnormal arch-artery patterning was also present (7/10), with mutants exhibiting no brachiocephalic artery, a shortened distance between the left common carotid and left subclavian artery, and other defects. This constellation of defects is similar to those seen in *Shh$^{–/–}$* mutants, representing fourth and sixth arch-artery defects (Fig. 1 and data not shown).

Histological analysis of four near-term *Nkx2.5$^{Cre/+}$; Shh$^{flox/–}$* double mutants confirmed the presence of a single OFT. Additionally, a complete atrio-ventricular septal defect was observed in each mutant (Fig. 1G′,H′). These defects are consistent with histological analysis of *Shh$^{–/–}$* embryos (Washington Smoak et al., 2005). These data demonstrate that loss of *Shh* function within the *Nkx2.5$^{Cre}$* domain is sufficient to recapitulate the OFT, arch-artery and intra-cardiac defects observed in *Shh$^{–/–}$* mutants. Finally, when we ablated *Shh* from the AHF (the major non-endodermal domain of *Nkx2.5$^{Cre}$*) using *Mef2C-AHF-Cre* (Verzi et al., 2005), we detected no OFT defects (data not shown), supporting our model that endodermal SHH is necessary for OFT development.

## Abnormal early OFT and right ventricle development in *Nkx2.5$^{Cre/+}$; Shh$^{flox/–}$* mutant embryos

We next examined *Nkx2.5$^{Cre/+}$; Shh$^{flox/–}$* mutant embryos at earlier stages to determine the cause and timing of the OFT defects. Lengths of both the OFT and right ventricle were compared between mutant E10.5 embryos and littermates. Mutants displayed obvious OFT and right ventricle shortening (Fig. 2A-D,G). The OFT and right ventricle were reduced, on average, by 20 and 15%, respectively (Fig. 2A-D, black bars, Fig. 2G), whereas the left ventricle was not statistically different in size (Fig. 2A,B, white bar). These data imply a role for endodermally-derived SHH in the elongation of the OFT and, therefore, in AHF development.

At E10.5, the OFT conotruncal cushions were already distinct bulges populated by CNCCs. We carried out fluorescent-confocal imaging for the endothelial marker PECAM-1 (Fig. 2E,F), and histological analysis (Fig. 2E′,F′) of *Nkx2.5$^{Cre/+}$; Shh$^{flox/–}$* mutant and control embryos. While mesenchyme was present, distinct OFT cushions were poorly formed and small, suggesting a deficit

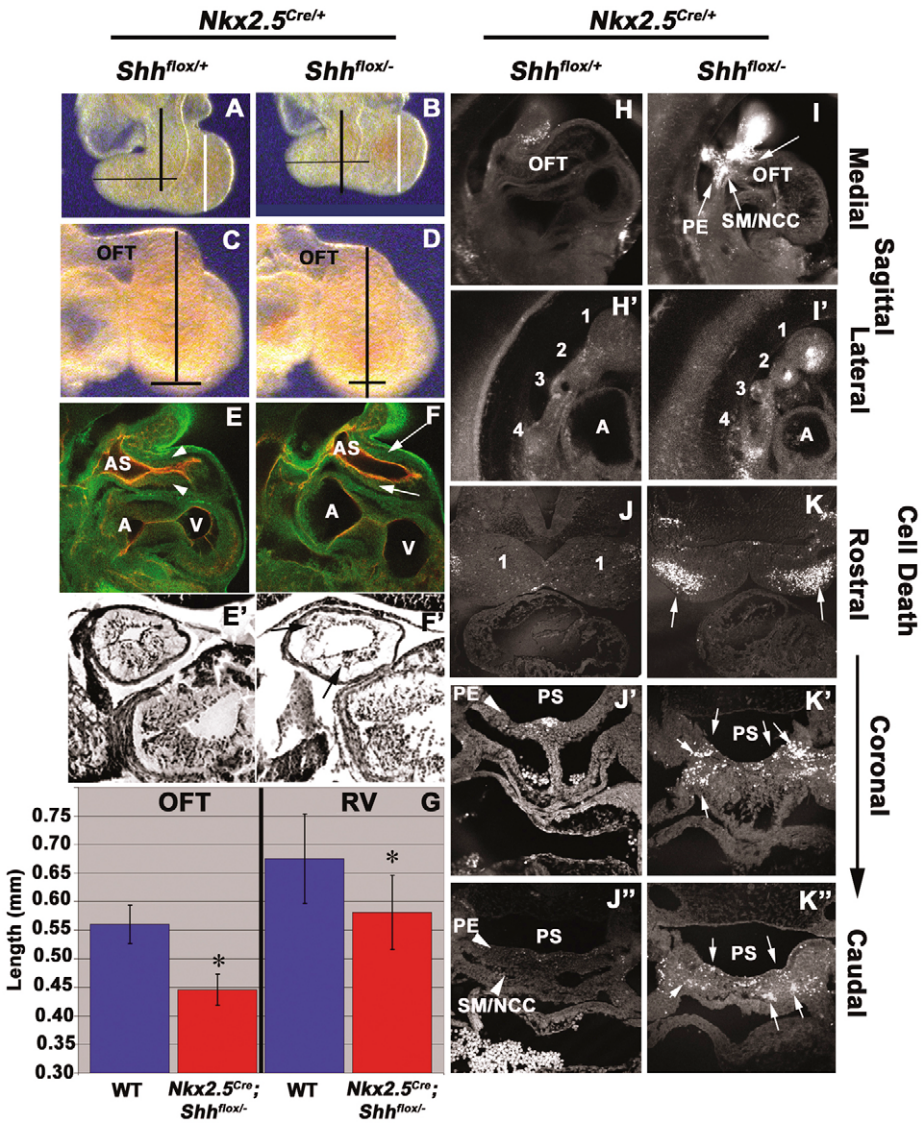


**Fig. 2. OFT lengthening and conotruncal cushion development is abnormal in *Nkx2.5*$^{Cre/+}$; *Shh*$^{flox/–}$ embryos due to cell death.** (**A-D**) Comparing E10.5 OFT and right ventricle length between wild-type (A,C) and *Nkx2.5*$^{Cre/+}$; *Shh*$^{flox/–}$ (B,D) embryos reveals a reduction in length of the mutant OFT and right ventricle (all bars are identical in adjacent images and quantified in **G**), whereas the left ventricle is unchanged. Paired *t*-test $P$=0.002 for OFT and $P$=0.025 for the right ventricle. (**E-F′**) OFT conotruncal cushions (F,F′, arrows) are reduced at E10.5 compared with *Nkx2.5*$^{Cre/+}$; *Shh*$^{flox/+}$ (E,E′). Immunohistochemistry markers in E and F are PECAM (red) and AP2α (green). (**H-K″**) Levels of cell death, as revealed by Lysotracker Red analysis, at E10.5 (H-I′, sagittal views; J-K″, frontal views) demonstrate increased cell death in the pharyngeal endoderm (K,K′), in the splanchnic mesoderm (I,K′) and within the core-arch mesoderm (I′) of mutants. In all panels, arrows and arrowheads mark abnormal and normal findings, respectively, in mutants as compared with control embryos. A, atrium; OFT, outflow tract; PE, pharyngeal endoderm; SM/NCC, splanchnic mesoderm/neural crest cells; V, ventricle; PS, pharyngeal space; 1-4, pharyngeal arch 1-4.

in CNCCs (Fig. 2E-F′). Finally, the aorticopulmonary septum within the aortic sac failed to form by E10.5 (data not shown). These data imply a role for endodermal SHH in CNCC development as well as in AHF development.

## Increased pharyngeal cell death in *Nkx2.5*$^{Cre/+}$; *Shh*$^{flox/–}$ embryos

To determine why the AHF and CNCCs are deficient in these mutant embryos, we tested for increased cell death and/or reduced cellular proliferation. Lysotracker Red fluorescent probe demonstrated increased levels of cell death at E9.5 and E10.5 in all *Nkx2.5*$^{Cre/+}$; *Shh*$^{flox/–}$ embryos tested, compared with controls (Fig. 2H-K″). High levels of cell death were observed in the splanchnic mesoderm and/or CNCCs located ventral to the pharyngeal endoderm and posterior to the OFT (putative AHF cells) (Fig. 2H,I,K′,K″). Interestingly, an increase in cell death was also observed in the pharyngeal arches, with particularly high levels specifically in the presumptive core arch mesoderm, a tissue identified as a component of the AHF at earlier stages, but which, at these stages, is a precursor to craniofacial muscle groups (Fig. 2H′,I′,J,J′). Minimal levels of cell death were observed within the OFT itself at E10.5 (data not shown). Finally, increased levels of cell death were observed within the pharyngeal endoderm (Fig. 2I,K′,K″), indicating not only a survival requirement for SHH in the AHF and NCC, but in the pharyngeal endoderm as well.

Cell-proliferation studies at E9.5 using an antibody against phosphorylated histone H3 revealed no difference in the number of cells in mitosis within the splanchnic mesoderm or in the pharyngeal endoderm compared to controls (data not shown). Therefore, the overall increase in cell death in the AHF is probably the main factor contributing to the shortened OFT–right-ventricle phenotype observed in the mutants.

## Arch-artery development requires endodermal *Shh* expression

*Shh*$^{–/–}$ mutants have defective NCC migration, resulting in the abnormal development of many NCC derived structures (Washington Smoak et al., 2005). As a possible explanation for the CNCC deficits in *Shh*$^{–/–}$ embryos, loss of ventral neural tube expression of *Shh* could be the sole factor affecting NCC migration. Alternatively, the early requirement for *Shh* in the neural tube of the embryo may be masking

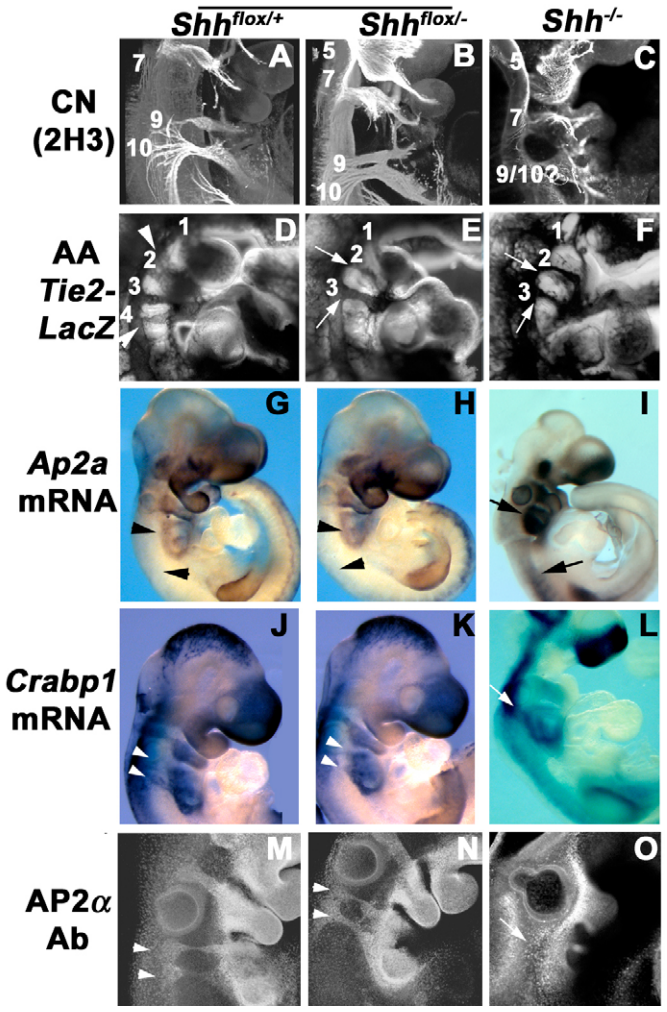


**Fig. 3. Cardiovascular, but not other neural crest-dependent, derivatives are affected by loss of endodermal *Shh*.** Comparison of wild-type, *Nkx2.5*$^{Cre/+}$; *Shh*$^{flox/-}$ and *Shh*$^{-/-}$ embryos reveals that only certain NCC-derived structures depend on endodermal *Shh*. (**A-F**) Cranial nerves (CN) are relatively normal in *Nkx2.5*$^{Cre/+}$; *Shh*$^{flox/-}$ embryos (B) compared with *Shh*$^{-/-}$ mutants (C), whereas their arch-artery patterning (E) more closely resembles *Shh*$^{-/-}$ defects (F) rather than wild-type (A,D). (**G-O**) Similarly, expression of the NCC markers *Ap2α* and *CrabP1*, as well as AP2α antibody, in *Nkx2.5*$^{Cre/+}$; *Shh*$^{flox/-}$ mutants (H,K,N) resemble wild-type (G,J,M) and not the abnormal pattern seen in *Shh*$^{-/-}$ embryos (I,L,O). In all panels, arrows and arrowheads mark abnormal and normal findings, respectively, in mutants as compared with control embryos.

a direct or indirect role for *Shh* in the pharyngeal endoderm. Therefore, we examined the development of several NCC derivatives in *Nkx2.5*$^{Cre/+}$; *Shh*$^{flox/-}$ mutant embryos.

The NCC-derived cranial neurofilaments of *Shh*$^{-/-}$ embryos were highly disorganized at E10.5, as observed using the 2H3 neurofilament antibody (Fig. 3C). However, we did not detect significant differences in neurofilament organization between wild-type and *Nkx2.5*$^{Cre/+}$; *Shh*$^{flox/-}$ embryos (Fig. 3A,B), although minor defects in cranial nerve patterning could not be ruled out.

Another important role for NCCs is to support arch-artery development. Using two methods, endothelial cell detection via the *Tie2-lacZ* allele (Fig. 3D-F) and via India-ink injections at E10.5 (data not shown), we detected fourth and sixth arch-artery defects consistent with the terminal arch-artery pattern defects described for *Nkx2.5*$^{Cre/+}$; *Shh*$^{flox/-}$ mutant embryos and similar to *Shh*$^{-/-}$ embryos (Fig. 3D-F). *Tie2-lacZ*-positive cells were observed in mutant embryos where the fourth arch-artery should form, but a well-formed artery, patent to ink, was not observed (data not shown). These results indicate that *Shh* expression within the *Nkx2.5*$^{Cre}$ domain is required for arch-artery patterning but not for grossly normal neuroganglia development.

A contributing factor to the OFT and pharyngeal arch defects observed in *Shh*$^{-/-}$ embryos is the abnormal early NCC migration and subsequent increased levels of NCC death. We examined multiple NCC markers in *Nkx2.5*$^{Cre/+}$; *Shh*$^{flox/-}$ mutants to determine whether NCC migration is altered. Whole-mount in situ analysis of *AP2α* and *CrabP1* demonstrated that, at E10.5, the expression patterns of NCC markers in the dorsal portion of mutant embryos were similar to those of wild-type embryos. This is in stark contrast to the expression patterns in *Shh*$^{-/-}$ embryos (Fig. 3G-L). Whole-mount immunofluorescent analysis of AP2α protein did reveal subtle migratory disorganization of the neural crest in both post-otic streams of *Nkx2.5*$^{Cre/+}$; *Shh*$^{flox/-}$ mutants, but this was minor compared with the defects seen in *Shh*$^{-/-}$ embryos (Fig. 3M-O). These data indicate that neural tube and/or notochord *Shh*, but not pharyngeal endoderm *Shh*, expression is most probably required for normal early NCC migration; by contrast, endodermal *Shh* is required for pharyngeal survival of NCCs.

## NCCs require endogenous Hh signaling for OFT septation

Loss of endodermal *Shh* results in abnormal AHF and CNCC development. As stated earlier, previous studies have suggested a possible interaction between these two fields of cells. To determine whether endodermal SHH is acting directly or indirectly on these two populations of cells, we performed further tissue-specific loss-of-function studies. The obligate Hh receptor *Smo* is expressed throughout the developing embryo (Zhang et al., 2001). Loss of *Smo* from a responding cell results in the complete inactivation of all Hh signaling pathways (Zhang et al., 2001). *Smo* homozygous null mutants die at approximately E9.5 with a variety of defects, including defective cardiac tube formation (Zhang et al., 2001). To address whether CNCCs directly respond to Hh signaling during cardiovascular development, we conditionally ablated *Smo* using the NCC-specific Cre recombinase *Wnt1-Cre*.

Although previous studies have characterized the striking craniofacial defects of *Wnt1-Cre; Smo*$^{flox/null}$ mutant embryos, cardiac defects were not described (Jeong et al., 2004). We determined that *Wnt1-Cre; Smo*$^{flox/-}$ embryos survive to term with single OFT septation defects (17/23) and arch-artery defects. Remaining mutant embryos had partial septation of the OFT, resulting in either a hypoplastic pulmonary artery with an aberrant origin (4/23) or a complete separation of a transposed aorta and hypoplastic pulmonary artery (2/23) (Fig. 4A,B and data not shown). Neither of these phenotypes were observed in *Nkx2.5*$^{Cre/+}$; *Shh*$^{flox/-}$ nor *Shh*$^{-/-}$ mutants. These data support a direct role for Hh signaling in NCC development and that loss of this signal results in OFT defects similar, but not identical, to those observed after the complete loss of *Shh*.

## Reduced number and abnormal pattern of CNCCs within the OFT

To follow CNCCs, we crossed the Cre recombinase reporter *R26R* with *Smo*$^{flox2}$ females to generate *Wnt1-Cre; Smo*$^{flox/-}$; *R26R* mutant embryos. This method affords a pseudo-'NCC-lineage trace' by

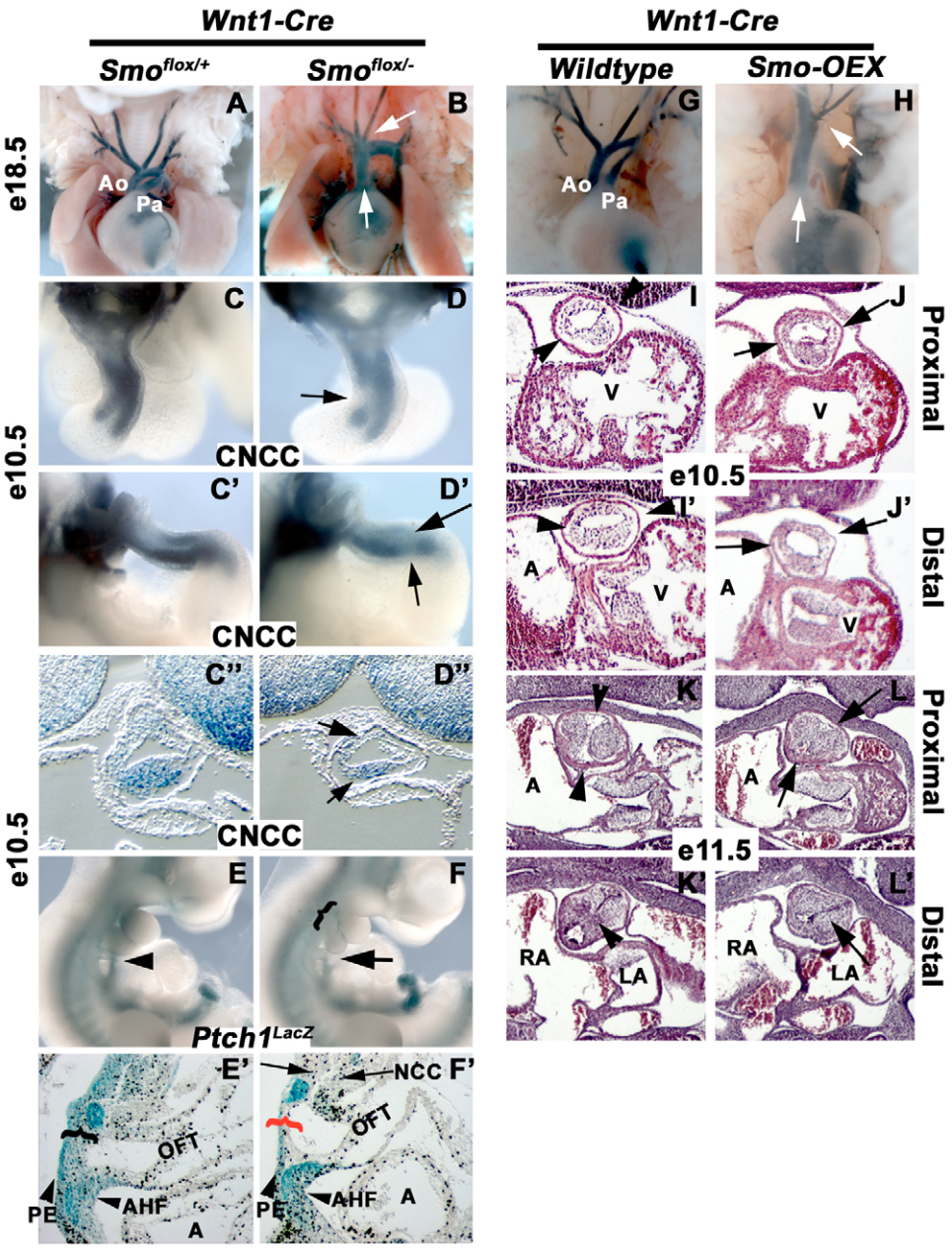


**Fig. 4. Ablation of Hh signaling within CNCCs results in a single OFT due to a reduced number of CNCCs.** (**A**,**B**) *Wnt1-Cre*-mediated ablation of *Smo* results in a single OFT and abnormal arch-artery patterning at E18.5 (B, arrows) compared with controls (A). (**C-D′**) NCC-lineage trace using the *R26R* reporter demonstrates a reduction in the total number, as well as abnormal localization, of CNCCs within the developing OFT at E10.5 (D,D′, arrows) compared with controls (C,C′). (**C″**,**D″**) Section analysis of C and D in the frontal plane reveals reduced cushion size (D″) compared with controls (C″). (**E-F′**) Reduction of Hh signaling is detected by the *Ptch1*$^{lacZ}$ activity shown in whole-mount (F) and sagittal (F′) sections compared with controls (E,E′). In *Wnt1-Cre; Smo*$^{flox/–}$ mutants, there is decreased activity within the pharyngeal arches (bracket, F) and dorsal to the aortic sac (arrow in F). (**G**,**H**) Constitutive activation of the Hh pathway within NCCs using *Smo*$^{OEX}$ also results in a single OFT (H versus G). (**I-L′**) Proximal/distal section analysis of *Wnt1-Cre; Smo*$^{OEX}$ embryos at E10.5 (J,J′) and E11.5 (L,L′) reveals abnormal localization and the compaction of cells within the OFT (J,J′), and that, despite the presence of cushions, septation is not taking place (L,L′) when compared with controls at E10.5 (I,I′) and E11.5 (K,K′). In all panels, arrows and arrowheads mark abnormal and normal findings, respectively, in mutants as compared with control embryos. Ao, aorta; Pa, pulmonary artery; AS, aortic sac; AHF, anterior heart field; A, atrium; V, ventricle.

marking NCCs with Cre recombination. In wild-type embryos, CNCCs enter the OFT organized into two opposing streams that spiral along the length of the OFT. We analyzed NCC migration in *Wnt1-Cre; Smo*$^{flox/–}$*; R26R* mutants at E9.5, E10.5 and E11.5 by detection of β-galactosidase activity (β-gal) (Fig. 4C-D″ and data not shown). The overall number of CNCCs reaching the OFT in mutant embryos appeared to be moderately reduced (compare number of blue cells in Fig. 4C″ and D″). In addition, analysis suggested a lack of two distinct streams of CNCCs in the distal OFT (truncus) (Fig. 4D′), whereas gaps appeared in other areas of the OFT (Fig. 4D,D′, arrows).

Histological analysis at E10.5 revealed a reduction in CNCCs dorsal to the aortic sac and ventral to the pharyngeal endoderm, consistent with the patterns of cell death that were also observed in these mutants (data not shown). This CNCC population also contributed to the development of the aorticopulmonary septum within the aortic sac. While present in *Wnt1-Cre; Smo*$^{flox/–}$ embryos at E10.5, this structure was sparsely populated with CNCCs and was smaller than in somite-matched wild-type embryos (data not shown). These data indicate that CNCC contribution to the aorticopulmonary septum and OFT cushions requires direct Hh signaling.

Previously published data demonstrate that NCCs abnormally cross the midline ventral to the neural tube in *Shh*$^{–/–}$ embryos (Washington Smoak et al., 2005). This abnormal early NCC migration was not observed in *Wnt1-Cre; Smo*$^{flox/–}$ embryos (data not shown). Together, these data implicate a non-cell-autonomous repulsive effect of Hh signaling on early NCC migration and support a cell-autonomous effect for Hh signaling on pharyngeal NCCs.

## A subpopulation of CNCCs respond to Hh signaling

Previous study of *Shh*$^{–/–}$ mutants demonstrated that a majority of NCCs apparently do not express *Ptch1*$^{lacZ}$ (Washington Smoak et al., 2005). By contrast, our phenotypic analysis of the NCC genetic

**Table 1. Summary of the genetic experiments conducted and the resulting phenotypes**

| Cre used (gene deleted) | Domain of expression | Single OFT at E18.5 | Short OFT at E10.5 | Abnormal arch arteries at E10.5/E18.5 | AHF cell death | NCC death | Abnormal NCC localization/ septation defect |
|---|---|---|---|---|---|---|---|
| *Nkx2.5$^{Cre}$* (*Shh* or *Smo*) | PE, AHF, specified myocardium, endocardium | + | + | +/+ | + | + | +/+ |
| *Wnt1-Cre* (*Smo*) | NCCs | + | – | +/+ | – | + | ?/+ |
| *Mef2C-Cre* (*Smo*) | AHF | + | – | –/+ | – | – | –/+ |
| *TnT-Cre* (*Smo*) | Specified myocardium | – | – | –/– | ND | ND | ND |
| *Tie2-Cre* (*Smo*) | Endocardium | – | – | –/– | ND | ND | ND |

+, present; –, not present; ND, no data; ?, possibly; PE, pharyngeal endoderm; AHF, anterior heart field; NCC, neural crest cell.

ablation of *Smo* indicates that CNCCs are responding directly to Hh signaling. To investigate this apparent contradiction, we crossed the *Ptch1$^{lacZ}$* allele to *Smo$^{flox}$* females to generate mutants of the genotype *Wnt1-Cre; Smo$^{flox/–}$; Ptch1$^{lacZ}$*. This genetic strategy enables us to detect Hh responsiveness in a mutant background.

Embryos collected at E10.5 and stained for *lacZ* expression revealed a Hh-responsive CNCC sub-population dorsal to the aortic sac and ventral to the pharyngeal endoderm at the axial level of the OFT. In wild-type embryos, these cells had high levels of *Ptch1$^{lacZ}$* activity, which was reduced in *Wnt1-Cre; Smo$^{flox/–}$* mutant embryos (Fig. 4E-F, arrowhead). Histological analysis confirmed that cells are still present in this region in mutant embryos despite the loss of *Ptch1$^{lacZ}$* activity (Fig. 4E′-F′, arrows). This population was adjacent to splanchnic mesoderm, which remained positive for *Ptch1$^{lacZ}$* activity (Fig. 4E′,F′, arrowhead) in both wild-type and mutant embryos. In addition, there was a decrease in the number of *Ptch1$^{lacZ}$*-positive cells immediately dorsal to the aortic sac, consistent with the loss of some NCCs (Fig. 4E′,F′, brackets). As predicted by our *Cre* reporter expression, *Wnt1-Cre* elimination of *Smo* did not affect OFT myocardial, pharyngeal core arch or endodermal *Ptch1$^{lacZ}$* expression (Fig. 4E′,F′ and data not shown).

Finally, to confirm that the phenotype was due to loss of Smo from NCCs and not from other tissues, we used an additional NCC-specific *Cre* allele, *P0-Cre* (Yamauchi et al., 1999). *P0-Cre* elimination of *Smo* resulted in identical cardiac defects (data not shown), confirming that *Smo* is required in NCCs for OFT development.

## Localized Hh signaling to CNCCs is not required for cushion formation, but is necessary for OFT septation

Hh signaling directly to the CNCCs appears crucial for CNCC survival and population of the OFT. It is unclear whether endodermal Hh signaling is directly organizing CNCCs into forming opposing conotruncal OFT cushions before they enter the OFT, or whether the two lines of OFT myocardial Hh activity are necessary to guide the CNCCs within the OFT, as hypothesized in our previous study (Washington Smoak et al., 2005). To help address this, we used an inducible, constitutively activated *Smo* transgene (*Smo$^{OEX}$*) in combination with the NCC-specific *Cre* allele *Wnt1-Cre*. This cross results in continuous activation of the Hh signaling pathway in all NCCs. *Wnt1-Cre; Smo$^{OEX}$* embryos have previously been described as having striking craniofacial abnormalities that are consistent with NCC defects (Jeong et al., 2004). We found that surviving E15.5 mutants also had a single, patent OFT vessel (Fig. 4G,H). However, well-developed OFT cushions were observed at E10.5. The CNCC-derived cushion mesenchyme was more compact, probably due to differences in cell morphology, although an increased quantity of CNCCs could not be ruled out (Fig. 4I-J′). In addition, more CNCCs were observed in the cardiac jelly, where the endocardium and myocardium are usually in close proximity (Fig. 4I′,J′, arrows). Early analysis showed that approximately half of these mutants died at approximately E11.5 and that the OFT was not patent to ink (data not shown). This abnormal localization could result in the obstruction of the developing OFT. In addition, section analyses of surviving E11.5 *Wnt1-Cre; Smo$^{OEX}$* embryos clearly demonstrated a lack of cushion fusion in the distal OFT (Fig. 4K′,L′), whereas the more proximal OFT cushions were in closer approximation to each other (Fig. 4K,L). Together, these data demonstrate that CNCCs can populate the OFT cushions in the presence of continuous Hh signaling, but that later septation events are inhibited by such signaling. This result also supports the hypothesis that direct localized Hh signaling is required for normal CNCC localization within the OFT but not for population of the conotruncal cushions in general.

## The AHF directly requires intact Hh signaling for OFT septation but not for OFT lengthening

The OFT-shortening defects and increased cell death in *Shh$^{–/–}$* and *Nkx2.5$^{Cre/+}$; Shh$^{flox/–}$* embryos suggest that SHH has a role in AHF contribution to OFT development. Although the data presented above clearly demonstrates a direct requirement on CNCCs, SHH produced in the overlying pharyngeal endoderm may also influence the AHF either directly or indirectly. To determine whether Hh signaling directly to the AHF is required for normal OFT development, we conditionally ablated *Smo* from the AHF using *Mef2C-AHF-Cre* (referred to here as *AHF-Cre*) (Verzi et al., 2005). *AHF-Cre* is expressed in the splanchnic and core arch mesoderm, but is not expressed within the pharyngeal endoderm (see Fig. S1 in the supplementary material).

*AHF-Cre; Smo$^{flox/–}$* mutant embryos also had a single OFT (14/16) and abnormal arch-artery patterning (4/16) (see Table 1, Fig. 5A,B). Surprisingly, unlike *Nkx2.5$^{Cre/+}$; Shh$^{flox/–}$* mutants, we did not detect the same early defects of OFT lengthening in embryos lacking *Smo* specifically within the AHF (Fig. 5C-D′ and data not shown). OFT cushions appeared relatively normal, although a slightly reduced size could not be ruled out, as detected by both *Tie2-lacZ* β-gal staining and histological section analysis at E10.5 in *AHF-Cre; Tie2-lacZ; Smo$^{flox/–}$* embryos (Fig. 5C′,D′,E,F). Consistent with these findings and in contrast to the observed increase in cell apoptosis observed in *Nkx2.5$^{Cre/+}$; Shh$^{flox/–}$* embryos, there was no appreciable difference in cell death between wild-type and *AHF-Cre; Smo$^{flox/–}$* embryos at E10.5 (data not shown). Section analysis at E12.5 demonstrated that, although OFT cushions were present in *AHF-Cre; Tie2-LacZ; Smo$^{flox/–}$* mutants, no OFT septation had occurred (Fig. 5G-H').

To test the specificity of Hh signaling and where it was absent in these *AHF-Cre* knockouts, we also examined *AHF-Cre; Smo$^{flox/–}$; Ptch1$^{lacZ}$* mutants. Loss of *Ptch1$^{lacZ}$* expression was detected in AHF

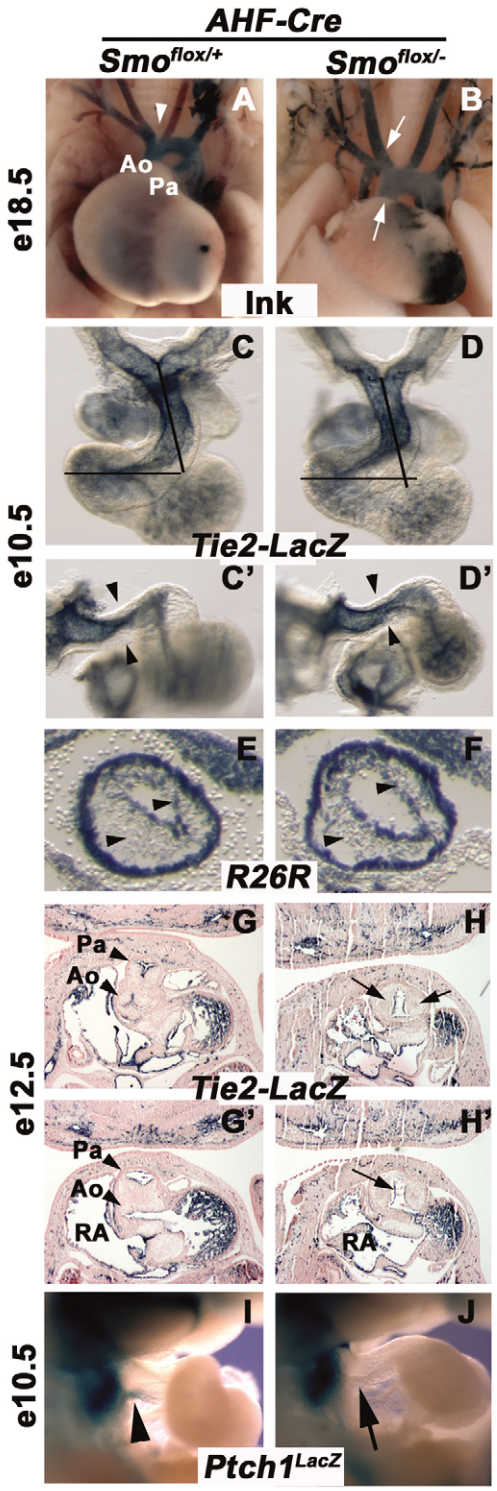


**Fig. 5. AHF ablation of Hh signaling results in a single OFT due to septation failure, but not in a shortened OFT.** (**A**,**B**) Ink injections of wild type (A) and *AHF-Cre; Smo*$^{flox/-}$ (B) at E18.5 reveals a single OFT in the mutants. (**C-F**) β-galactosidase staining in *AHF-Cre; Smo*$^{flox/-}$ mutants that are also transgenic for *Tie2-lacZ* reveals that the OFT is not significantly shortened (D,D′) and that cushions form (D′,F) similar to control (C,C′,E) embryos (bar length is identical in C,D). Arrowheads point to cushions compressing the endothelial channel in C′,D′. (E,F) Section analysis of E10.5 *AHF-Cre; Smo*$^{flox/-}$ mutants also transgenic for the *Cre* reporter *R26R* (F) reveals that CNCCs populate the OFT cushions in relatively normal numbers compared to controls (E). (**G-H′**) Although the cushions are well-formed at E12.5 (H,H′, arrows), septation does not complete in *AHF-Cre; Smo*$^{flox/-}$ mutants, resulting in a single OFT channel (H,H′) compared with controls (G,G′). (**I**,**J**) *Ptch1*$^{lacZ}$ expression in *AHF-Cre; Smo*$^{flox/-}$ mutants reveals a specific loss of expression within the AHF, including in the expression entering the OFT (J versus I, arrow). In all panels, arrows and arrowheads mark abnormal and normal findings, respectively, in mutants as compared with control embryos. Ao, aorta; Pa, pulmonary artery; OFT, outflow tract; RA, right atrium; LV, left ventricle.

cells only, specifically those that are continuous with the wall of the OFT (Fig. 5I,J and data not shown). Together, these data indicate that, although there is a similar single-OFT phenotype and also a direct role for Hh signaling via *Smo* in AHF cells, Hh is required in AHF-derived cells for a later septation step and not for AHF survival or OFT lengthening.

Finally, although E18.5 mutants showed defects in arch-artery patterning, arch-artery development appeared normal in *AHF-Cre; Tie2-lacZ; Smo*$^{flox/-}$ mutant embryos at E10.5 (8/8, data not shown). Therefore, Hh signaling within the AHF is not required for early arch-artery development, but has a later role in arch-artery patterning/remodeling. These data also indicate that some of the defects observed in *Nkx2.5*$^{Cre/+}$*; Shh*$^{flox/-}$ embryos cannot be explained by AHF or CNCC deficiencies alone.

## The endoderm requires Hh signaling cell-autonomously for OFT lengthening

To determine whether cell-autonomous *Smo* elimination from NCCs could also affect AHF development, we examined OFT lengthening. OFT length was indistinguishable between *Wnt1-Cre; Smo*$^{flox/-}$ mutant embryos and somite-matched wild-type littermates when compared at E10.5 (data not shown). This indicates that the reduction of OFT length observed in both *Shh*$^{-/-}$ and in *Nkx2.5*$^{Cre/+}$*; Shh*$^{flox/-}$ embryos is not due to a direct cell-autonomous effect on either CNCCs or on the AHF.

What tissue is responsible? SHH can diffuse unknown distances and, therefore, several candidate tissues remain. In order to address this question, we first tested whether cells in the *Nkx2.5* domain itself require *Smo* cell-autonomously for OFT lengthening. To do this, we generated *Nkx2.5*$^{Cre/+}$*; Smo*$^{flox/-}$ mutants (see Materials and methods). Informatively, these mutants have a single OFT and an OFT shortening similar to *Shh*$^{-/-}$ embryos, indicating either that a non-NCC and non-AHF cell population within the *Nkx2.5* domain requires Hh signaling for OFT lengthening, or that a combination of AHF and NCC Hh signaling is required for OFT lengthening.

We have identified three significant differences between *Nkx2.5*$^{Cre}$ and *AHF-Cre* expression that may account for why *Nkx2.5*$^{Cre/+}$*; Smo*$^{flox/-}$ mutants, but not *AHF-Cre; Smo*$^{flox/-}$ mutants, have a greatly shortened OFT. Besides the AHF, *Nkx2.5*$^{Cre}$ is expressed in the pharyngeal endoderm, primary heart field and endocardium (a small population of endocardium appears positive in *Nkx2.5*$^{Cre}$*; R26R* embryos that is not positive in *AHF-Cre; R26R* embryos) (see Fig. S1 in the supplementary material; data not shown). To test which of these three populations of cells is required for AHF survival and OFT lengthening, we generated two additional classes of *Smo* mutants.

The first is a myocardial-specific (*TnT-Cre*) mutant, in order to rule out the primary heart field. These mutants have normal OFT septation and length and a normal OFT phenotype at birth.

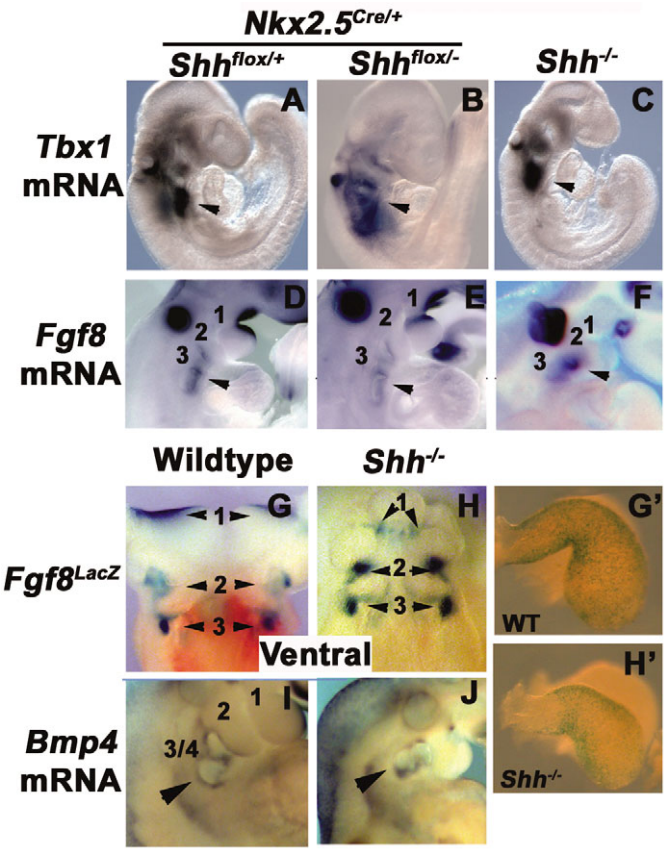


**Fig. 6. Endodermal *Tbx1*, *Fgf8* and *Bmp4* expressions appear normal in mutants.** (**A-C**) In situ analysis for *Tbx1* at E9.5 in *Nkx2.5*$^{Cre/+}$; *Shh*$^{flox/-}$ (B) and *Shh*$^{-/-}$ (C) mutants appears normal within the pharyngeal endoderm when compared to control (A). (**D-F**,**I**,**J**) Similarly, mRNA levels for *Fgf8* (D-F) and *Bmp4* (I,J) also appear normal. (**G-H'**) *Fgf8*$^{lacZ}$ expression is also grossly normal in *Shh*$^{-/-}$ pharyngeal endoderm (H) and OFT/right ventricle (H') when compared to controls (G,G').

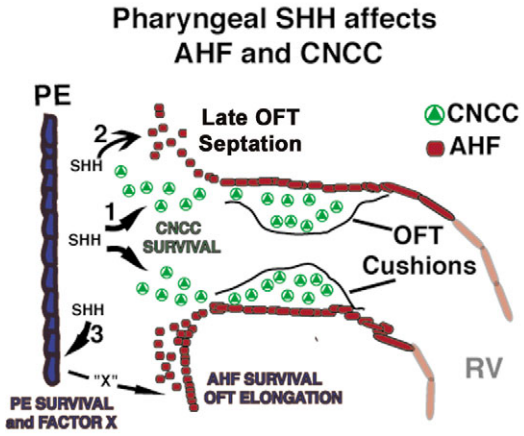


**Fig. 7. Model of Hh signaling during OFT development.** Pharyngeal-derived (PE) SHH performs three main roles. First (1), SHH acts as a direct survival factor to CNCCs. Second (2), in AHF-derived myocardium, SHH acts via *Smo* to provide a patterning signal that is required for an unknown function in completing septation between E10.5 and E12.5. Third (3), SHH is a direct survival factor for the pharyngeal endoderm, and its loss results in the absence of a secondary signal ("X") necessary for AHF survival and for the lengthening of the OFT. Disruption of any of these processes either alone or in combination can result in a single-OFT phenotype, via different mechanisms. RV, right ventricle.

The second class was an endocardial knockout using *Tie2-Cre*. Again, these mutants did not have OFT septation or shortening defects (see Fig. S2A-C in the supplementary material; data not shown).

Finally, even though we cannot detect *Shh* expression within the developing heart by mRNA in situ analysis, we tested whether low levels of SHH may be produced within the heart. We generated RNA from whole hearts between E9.5 and E12.5, and performed reverse transcriptase (RT)-PCR for *Shh*. We were unable to detect *Shh* expression at 30 cycles [we could not rule out low levels of expression because, at 35 cycles of RT-PCR, a faint band was detected in some samples at these stages (see Fig. S2D in the supplementary material)]. Together, these genetic experiments demonstrate that deletion of *Smo* in either the myocardium or the endocardium alone does not affect OFT lengthening (Table 1). We propose that SHH produced from pharyngeal endoderm signals to the endoderm in an autocrine fashion between E9.5 and E10.5 and that it is required for AHF survival and OFT lengthening. These data therefore raise the question that if SHH signals via SMO in the pharyngeal endoderm to produce a second signal for OFT lengthening, what is that signal?

### *Tbx1* is induced in both *Shh*$^{-/-}$ and *Nkx2.5*$^{Cre/+}$; *Shh*$^{flox/-}$ embryos

*Tbx1* is a transcription factor within the DiGeorge syndrome critical-deletion region. Several studies have suggested that *Tbx1* is regulated by SHH via forkhead box (Fox) transcription factors within the pharyngeal arches (Garg et al., 2001; Yamagishi et al., 2003). In situ hybridization was performed to determine whether *Tbx1* is downregulated in *Nkx2.5*$^{Cre/+}$; *Shh*$^{flox/-}$ mutant embryos at E9.5, prior to the appearance of the mutant pharyngeal arch phenotype. No differences in expression pattern or intensity of pharyngeal endoderm expression were observed between mutant and wild-type littermates (Fig. 6A,B). As original *Tbx1* in situ studies focused on *Shh*$^{-/-}$ embryos at E10.5 and later stages (Garg et al., 2001), we sought to determine whether a difference in *Tbx1* expression could be observed in *Shh*$^{-/-}$ embryos at E9.5. By whole-mount in situ hybridization, we found that E9.5 *Shh*$^{-/-}$ embryos had *Tbx1* endodermal expression patterns consistent with wild-type littermates (Fig. 6C). These data, combined with previous studies, suggest that SHH is not required for pharyngeal endodermal *Tbx1* induction.

Two potential ligands expressed in the pharyngeal endoderm and implicated in OFT lengthening are *Fgf8* and *Bmp4*. *Fgf8* is expressed both within the AHF and in the pharyngeal endoderm, and has been implicated in AHF and NCC development (Ilagan et al., 2006; Park et al., 2006). We examined the in situ expression of *Fgf8* in *Nkx2.5*$^{Cre/+}$; *Shh*$^{flox/-}$ mutant embryos and *Shh*$^{-/-}$ mutant embryos at E10.5, and compared them to E10.5 controls (Fig. 6D-F): no significant expression differences were detected. To confirm this finding, we also examined the expression of *Fgf8*$^{lacZ}$ (Ilagan et al., 2006) in *Shh*$^{-/-}$ embryos and detected no significant differences in

pharyngeal endoderm expression (Fig. 6G,H). However, there was a reduced number of β-galactosidase-positive cells in the developing OFT and right ventricle of *Shh*$^{-/-}$ mutants, which we attributed to the reduction of these tissues and not to a loss of expression (Fig. 6G′,H′). Finally, we did not detect a significant loss of *Bmp4* expression within the pharyngeal endoderm (Fig. 6I,J). If there is a secondary endodermal signal induced by SHH for OFT lengthening, it is not likely to be mediated by transcriptional changes in either *Fgf8* or *Bmp4*. In addition, these data demonstrate that the pharyngeal endoderm is specified and fairly normal at these stages in *Shh*$^{-/-}$ embryos, as evinced by the relatively normal expression of *Bmp4*, *Fgf8* and *Tbx1*.

## DISCUSSION

Previous studies have implicated Hh signaling in various aspects of heart development, from the early induction of cardiac progenitors and left-right axis determination to its direct roles in cardiac morphogenesis. This work indicates a direct role for endodermal SHH signaling on OFT and arch-artery patterning. Moreover, it demonstrates that the AHF, CNCCs and the pharyngeal endoderm all require Hh signaling directly. Previous work on OFT development has primarily focused on the signaling and genetic requirements of the AHF and CNCCs independently; here, we identify a common signaling pathway that affects both fields directly in their contribution to a common process, OFT septation. Additionally, this work confirms a role for AHF development in OFT septation separate from its previously defined role in OFT lengthening.

### Endodermal Shh is required for cardiac development

This work reveals SHH as a key signaling molecule that mediates a long-suspected role for endodermal tissues in late cardiac formation (Fig. 7). In addition to the previously appreciated role for *Shh* in foregut development (Litingtung et al., 1998), these data are unique in demonstrating a direct requirement in heart development. Using *Nkx2.5*$^{Cre}$ to conditionally ablate *Shh*, we recapitulated the cardiac defects observed in *Shh*$^{-/-}$ embryos. Although the only recognized domain of *Shh* expression overlapping with *Nkx2.5*$^{Cre}$ is the pharyngeal endoderm, we cannot rule out additional, uncharacterized domains that may contribute to cardiac development, particularly within the developing atria. We are unable to detect significant *Shh* expression by RT-PCR within the heart between E9.5 and E10.5 (the timeframe in which the AHF and CNCCs appear to be dying), supporting our contention that the pharyngeal endoderm itself is the primary source of SHH. Eliminating *Shh* with the myocardial-specific *TnT-Cre* or in the AHF domain using *AHF-Cre* results in no OFT defects, supporting the idea that the endoderm is the crucial SHH signaling source. The development and use of an early, endodermal-specific *Cre* transgene would be useful to confirm this finding.

### Hh signaling within the endoderm is required for AHF development

Previous work on *Shh*$^{-/-}$ mutants implicated the AHF as a direct target of SHH signaling. Although we confirmed that the AHF does require the signal in a cell-autonomous manner, we were surprised to find that it is required for OFT septation but not for OFT elongation. These data indicate that direct signaling to the AHF is not required for its survival or for OFT lengthening. Instead, we hypothesize that the pharyngeal endoderm itself has a requirement for SMO in an autocrine fashion, and that AHF survival is dependent on an unknown secondary signal from the endoderm. Neither *Fgf8* nor *Bmp4* appear to be this signal, because their expression does not appear to be altered in *Shh*$^{-/-}$ mutants.

In support of this hypothesis, we generated mutant mice of the genotype *Nkx2.5*$^{Cre/+}$*; Smo*$^{flox/-}$, in which the AHF, the primary heart field and the pharyngeal endoderm all lack Hh receptiveness. These embryos also displayed increased levels of AHF cell death and significant OFT and right ventricle shortening (data not shown). Consistent with our results, the OFT shortening resulting from *Isl1-Cre; Smo* elimination appears much milder compared with *Shh*$^{-/-}$ embryos (Lin et al., 2006). These authors report that *Isl1-Cre* is restricted to cardiac precursors and that *Shh* expression within pharyngeal endoderm is maintained. Any differences between our findings and those of Lin et al. could be due to different expression domains for *Mef2C-AHF-Cre* (*AHF-Cre*) and *Isl1-Cre*, or to the fact that *Isl1-Cre* is a heterozygous null. Additionally, the images provided for this particular line (Yang et al., 2006) suggest that *Isl1-Cre* includes tissues other than AHF cells (left ventricle, for example). Using the same *Isl1-Cre* as first reported by Cai et al. (Cai et al., 2003), we found that this transgenic line has incomplete and inconsistent expression within the AHF, which may explain why *Mef2C-AHF-Cre; Smo*$^{flox/-}$ embryos have differences in phenotype compared with the *Isl1-Cre; Smo*$^{flox/-}$ embryos. We therefore conclude that the AHF does not require *Smo* for the majority of OFT lengthening or for AHF survival. Rather, it appears that expression of *Smo* within the AHF is required for a latter stage of septation, between E10.5 and E12.5.

So what is the direct role of *Smo* within the AHF domain on OFT septation? Based on our analysis, we favor three possibilities. First, endocardial or myocardial *Smo* may be required for cushion fusion (Fig. 5G-H′and data not shown). Second, *Smo* may be required for the process of OFT myocardialization. Another possible role is in maintaining the proper cushion positioning within the developing OFT (Fig. 5). Loss of *Smo* from the developing AHF results in loss of *Ptch1*$^{lacZ}$ expression in the OFT myocardium (Fig. 5I,J). We previously hypothesized that this *Ptch1* expression may be required for the guidance of CNCCs (Washington Smoak et al., 2005), and it was also implicated in this role by Lin et al. (Lin et al., 2006). We do not favor this last possibility because we were unable to demonstrate consistent abnormal positioning of the CNCCs/cushions as seen in our reported results for *Shh*$^{-/-}$ embryos. In any case, the requirement of the AHF for Hh signaling occurs prior to the addition of this field to the OFT, because ablation of *Smo* from the myocardium of the OFT (*TnT-Cre; Smo*$^{flox/-}$) did not recapitulate the septation defect. Together, these data implicate both an indirect (endodermally elicited survival) and a direct (late septation) role for pharyngeal endoderm SHH signaling on the derivatives of the AHF.

### CNCCs, but not other NCCs, directly require endodermal SHH for survival

Another surprising result in these studies is that CNCCs require SHH directly for their survival. Our previous work indicated little, if any, expression of the downstream target *Ptch1*$^{lacZ}$ in CNCCs. Our *Wnt1-Cre; Smo*$^{flox/-}$ results clearly indicate that, contrary to our earlier interpretations, there is a cell-autonomous requirement for *Smo* within CNCCs. Loss of *Smo* resulted in the loss of CNCCs, with reduced OFT cushions and septation defects later in development. This requirement for endodermally-derived SHH did not extend to other distal NCCs, such as cranial nerve or dorsal root ganglia derivatives, because these structures were relatively normal when compared with *Shh*$^{-/-}$ embryos. Presumably, these structures are patterned by the midline neural expression of *Shh*. Analysis of

*Ptch1*$^{lacZ}$ expression in *Wnt1-Cre; Smo*$^{flox/-}$ embryos found a small region of CNCCs that were negative for *lacZ* just ventral to the endoderm and near the aortic sac. Most probably, the loss of signaling to this and earlier populations of CNCCs is responsible for the observed reduction in OFT cushions and for aorticopulmonary septum defects. However, we cannot rule out additional regions of Hh signaling to the CNCCs that are not detectable using the *Ptch1*$^{lacZ}$ allele.

Previous work in chick has suggested that NCC ablation can affect OFT lengthening (Hutson et al., 2006; Yelbuz et al., 2002). However, we did not detect a significant change in OFT length or in AHF cell death in *Wnt1-Cre; Smo*$^{flox/-}$ embryos, indicating that, if NCCs do influence OFT lengthening in the mouse, it is not via a Hh-dependent pathway. However, changes in CNCCs alone can result in late OFT defects that are independent of OFT lengthening defects. At this time, we cannot rule out that combinatorial loss of *Smo* from both the AHF and CNCCs would result in a shortened OFT.

## Similar phenotype, different mechanism?

Prior work investigating the OFT defects of *Shh*$^{-/-}$ mutant mice, and the conditional ablation studies described here, illustrate deficits in both the AHF and CNCCs due to a loss of Hh signaling. Additionally, ablation of *Smo* from either the AHF or from the CNCCs also results in abnormal septation. Although most near-term mutants of both types demonstrate completely unseptated OFTs, several 'escapers' were observed that indicate that the etiologies of the septation defect are not identical in these mutant classes. Several embryos of the genotype *Wnt1-Cre; Smo*$^{flox/-}$ were found to have partially-septated OFTs with hypoplastic pulmonary arteries, whereas several *AHF-Cre; Smo*$^{flox/-}$ mutants demonstrated a septated OFT with a severely hypoplastic aorta (data not shown). Although early (E10.5) defects are detected in the cushions of *Wnt1-Ce; Smo*$^{flox/-}$ embryos, OFT development was fairly normal in E10.5 *AHF-Cre; Smo*$^{flox/-}$ mutants. These data are consistent with the idea that failure to septate the OFT results from early defects in OFT cushion formation, aorticopulmonary septum development, late cushion fusion and, possibly, OFT lengthening, or some combination thereof.

In summary, we uncovered multiple roles for endodermal Hh in OFT development. Use of conditional genetics allowed us to reveal the different effects of signal loss to the AHF, to CNCCs and, by process of elimination, to the endoderm. Differing genetic perturbations resulted in similar term defects, stressing the interdependence of the development of each OFT component on the other components. Future studies will be required to elucidate the downstream genetic components regulated in each tissue and the mechanism controlling late OFT septation.

The authors would like to thank B. Black and K. Jiao for *Mef2c-AHF-Cre* and *TnT-Cre*, respectively. We also thank B. Patton and D. Malone for technical assistance. We thank B. Hogan, M. Choi and members of our laboratory for helpful critique of this manuscript. This work was supported by the NIH grants HD480305 and HL086853 to E.N.M. and Predoctoral AHA Grant #061543OU to M.M.G.

### Supplementary material

Supplementary material for this article is available at
http://dev.biologists.org/cgi/content/full/134/8/1593/DC1

### References

**Abu-Issa, R., Smyth, G., Smoak, I., Yamamura, K. and Meyers, E. N.** (2002). Fgf8 is required for pharyngeal arch and cardiovascular development in the mouse. *Development* **129**, 4613-4625.

**Brown, C. B., Wenning, J. M., Lu, M. M., Epstein, D. J., Meyers, E. N. and Epstein, J. A.** (2004). Cre-mediated excision of Fgf8 in the Tbx1 expression domain reveals a critical role for Fgf8 in cardiovascular development in the mouse. *Dev. Biol.* **267**, 190-202.

**Cai, C. L., Liang, X., Shi, Y., Chu, P. H., Pfaff, S. L., Chen, J. and Evans, S.** (2003). Isl1 identifies a cardiac progenitor population that proliferates prior to differentiation and contributes a majority of cells to the heart. *Dev. Cell* **5**, 877-889.

**Chapman, D. L., Agulnik, I., Hancock, S., Silver, L. M. and Papaioannou, V. E.** (1996). Tbx6, a mouse T-Box gene implicated in paraxial mesoderm formation at gastrulation. *Dev. Biol.* **180**, 534-542.

**Chiang, C., Litingtung, Y., Lee, E., Young, K. E., Corden, J. L., Westphal, H. and Beachy, P. A.** (1996). Cyclopia and defective axial patterning in mice lacking Sonic hedgehog gene function. *Nature* **383**, 407-413.

**Crossley, P. H. and Martin, G. R.** (1995). The mouse Fgf8 gene encodes a family of polypeptides and is expressed in regions that direct outgrowth and patterning in the developing embryo. *Development* **121**, 439-451.

**Danielian, P. S., Muccino, D., Rowitch, D. H., Michael, S. K. and McMahon, A. P.** (1998). Modification of gene activity in mouse embryos in utero by a tamoxifen-inducible form of Cre recombinase. *Curr. Biol.* **8**, 1323-1326.

**Echelard, Y., Epstein, D. J., St-Jacques, B., Shen, L., Mohler, J., McMahon, J. A. and McMahon, A. P.** (1993). Sonic hedgehog, a member of a family of putative signaling molecules, is implicated in the regulation of CNS polarity. *Cell* **75**, 1417-1430.

**Ferguson, C. A. and Graham, A.** (2004). Redefining the head-trunk interface for the neural crest. *Dev. Biol.* **269**, 70-80.

**Garg, V., Yamagishi, C., Hu, T., Kathiriya, I. S., Yamagishi, H. and Srivastava, D.** (2001). Tbx1, a DiGeorge syndrome candidate gene, is regulated by sonic hedgehog during pharyngeal arch development. *Dev. Biol.* **235**, 62-73.

**Goodrich, L. V., Milenkovic, L., Higgins, K. M. and Scott, M. P.** (1997). Altered neural cell fates and medulloblastoma in mouse patched mutants. *Science* **277**, 1109-1113.

**Harvey, R. P.** (2002). Patterning the vertebrate heart. *Nat. Rev. Genet.* **3**, 544-556.

**Hogan, B.** (1994). *Manipulating the Mouse Embryo: A Laboratory Manual*. Plainview, NY: Cold Spring Harbor Laboratory Press.

**Hu, T., Yamagishi, H., Maeda, J., McAnally, J., Yamagishi, C. and Srivastava, D.** (2004). Tbx1 regulates fibroblast growth factors in the anterior heart field through a reinforcing autoregulatory loop involving forkhead transcription factors. *Development* **131**, 5491-5502.

**Hutson, M. R. and Kirby, M. L.** (2003). Neural crest and cardiovascular development: a 20-year perspective. *Birth Defects Res. C Embryo Today* **69**, 2-13.

**Hutson, M. R., Zhang, P., Stadt, H. A., Sato, A. K., Li, Y. X., Burch, J., Creazzo, T. L. and Kirby, M. L.** (2006). Cardiac arterial pole alignment is sensitive to FGF8 signaling in the pharynx. *Dev. Biol.* **295**, 486-497.

**Ilagan, R., Abu-Issa, R., Brown, D., Yang, Y. P., Jiao, K., Schwartz, R. J., Klingensmith, J. and Meyers, E. N.** (2006). Fgf8 is required for anterior heart field development. *Development* **133**, 2435-2445.

**Jeong, J., Mao, J., Tenzen, T., Kottmann, A. H. and McMahon, A. P.** (2004). Hedgehog signaling in the neural crest cells regulates the patterning and growth of facial primordia. *Genes Dev.* **18**, 937-951.

**Kelly, R. G. and Buckingham, M. E.** (2002). The anterior heart-forming field: voyage to the arterial pole of the heart. *Trends Genet.* **18**, 210-216.

**Kelly, R. G., Brown, N. A. and Buckingham, M. E.** (2001). The arterial pole of the mouse heart forms from Fgf10-expressing cells in pharyngeal mesoderm. *Dev. Cell* **1**, 435-440.

**Kirby, M. L. and Stewart, D. E.** (1983). Neural crest origin of cardiac ganglion cells in the chick embryo: identification and extirpation. *Dev. Biol.* **97**, 433-443.

**Kirby, M. L., Gale, T. F. and Stewart, D. E.** (1983). Neural crest cells contribute to normal aorticopulmonary septation. *Science* **220**, 1059-1061.

**Koni, P. A., Joshi, S. K., Temann, U.-A., Olson, D., Burkly, L. and Flavell, R. A.** (2001). Conditional vascular cell adhesion molecule 1 deletion in mice: impaired lymphocyte migration to bone marrow. *J. Exp. Med.* **193**, 741-754.

**Lewis, P. M., Dunn, M. P., McMahon, J. A., Logan, M., Martin, J. F., St-Jacques, B. and McMahon, A. P.** (2001). Cholesterol modification of sonic hedgehog is required for long-range signaling activity and effective modulation of signaling by Ptc1. *Cell* **105**, 599-612.

**Lin, L., Bu, L., Cai, C. L., Zhang, X. and Evans, S.** (2006). Isl1 is upstream of sonic hedgehog in a pathway required for cardiac morphogenesis. *Dev. Biol.* **295**, 756-763.

**Litingtung, Y., Lei, L., Westphal, H. and Chiang, C.** (1998). Sonic hedgehog is essential to foregut development. *Nat. Genet.* **20**, 58-61.

**Long, F., Zhang, X. M., Karp, S., Yang, Y. and McMahon, A. P.** (2001). Genetic manipulation of hedgehog signaling in the endochondral skeleton reveals a direct role in the regulation of chondrocyte proliferation. *Development* **128**, 5099-5108.

**Meyers, E. N., Lewandoski, M. and Martin, G. R.** (1998). An Fgf8 mutant allelic series generated by Cre- and Flp-mediated recombination. *Nat. Genet.* **18**, 136-141.

**Mitchell, P. J., Timmons, P. M., Hebert, J. M., Rigby, P. W. and Tjian, R.** (1991). Transcription factor AP-2 is expressed in neural crest cell lineages during mouse embryogenesis. *Genes Dev.* **5**, 105-119.

**Moore-Scott, B. A. and Manley, N. R.** (2005). Differential expression of Sonic hedgehog along the anterior-posterior axis regulates patterning of pharyngeal pouch endoderm and pharyngeal endoderm-derived organs. *Dev. Biol.* **278**, 323-335.
**Moses, K. A., DeMayo, F., Braun, R. M., Reecy, J. L. and Schwartz, R. J.** (2001). Embryonic expression of an Nkx2-5/Cre gene using ROSA26 reporter mice. *Genesis* **31**, 176-180.
**Neubuser, A., Peters, H., Balling, R. and Martin, G. R.** (1997). Antagonistic interactions between FGF and BMP signaling pathways: a mechanism for positioning the sites of tooth formation. *Cell* **90**, 247-255.
**Noden, D.** (1991). Origins and patterning of avian outflow tract endocardium. *Development* **111**, 867-876.
**Park, E. J., Ogden, L. A., Talbot, A., Evans, S., Cai, C. L., Black, B. L., Frank, D. U. and Moon, A. M.** (2006). Required, tissue-specific roles for Fgf8 in outflow tract formation and remodeling. *Development* **133**, 2419-2433.
**Schlaeger, T. M., Bartunkova, S., Lawitts, J. A., Teichmann, G., Risau, W., Deutsch, U. and Sato, T. N.** (1997). Uniform vascular-endothelial-cell-specific gene expression in both embryonic and adult transgenic mice. *Proc. Natl. Acad. Sci. USA* **94**, 3058-3063.
**Soriano, P.** (1999). Generalized lacZ expression with the ROSA26 Cre reporter strain. *Nat. Genet.* **21**, 70-71.
**Stoner, C. M. and Gudas, L. J.** (1989). Mouse cellular retinoic acid binding protein: cloning, complementary DNA sequence, and messenger RNA expression during the retinoic acid-induced differentiation of F9 wild type and RA-3-10 mutant teratocarcinoma cells. *Cancer Res.* **49**, 1497-1504.
**Verzi, M. P., McCulley, D. J., De Val, S., Dodou, E. and Black, B. L.** (2005). The right ventricle, outflow tract, and ventricular septum comprise a restricted expression domain within the secondary/anterior heart field. *Dev. Biol.* **287**, 134-145.
**Waldo, K., Zdanowicz, M., Burch, J., Kumiski, D. H., Stadt, H. A., Godt, R. E., Creazzo, T. L. and Kirby, M. L.** (1999). A novel role for cardiac neural crest in heart development. *J. Clin. Invest.* **103**, 1499-1507.
**Ward, C., Stadt, H., Hutson, M. and Kirby, M. L.** (2005). Ablation of the secondary heart field leads to tetralogy of Fallot and pulmonary atresia. *Dev. Biol.* **284**, 72-83.
**Washington Smoak, I., Byrd, N. A., Abu-Issa, R., Goddeeris, M. M., Anderson, R., Morris, J., Yamamura, K., Klingensmith, J. and Meyers, E. N.** (2005). Sonic hedgehog is required for cardiac outflow tract and neural crest cell development. *Dev. Biol.* **283**, 357-372.
**Xu, H., Morishima, M., Wylie, J. N., Schwartz, R. J., Bruneau, B. G., Lindsay, E. A. and Baldini, A.** (2004). Tbx1 has a dual role in the morphogenesis of the cardiac outflow tract. *Development* **131**, 3217-3227.
**Yamagishi, H., Maeda, J., Hu, T., McAnally, J., Conway, S. J., Kume, T., Meyers, E. N., Yamagishi, C. and Srivastava, D.** (2003). Tbx1 is regulated by tissue-specific forkhead proteins through a common Sonic hedgehog-responsive enhancer. *Genes Dev.* **17**, 269-281.
**Yamauchi, Y., Abe, K., Mantani, A., Hitoshi, Y., Suzuki, M., Osuzu, F., Kuratani, S. and Yamamura, K.** (1999). A novel transgenic technique that allows specific marking of the neural crest cell lineage in mice. *Dev. Biol.* **212**, 191-203.
**Yang, L., Cai, C., Lin, L., Qyang, Y., Chung, C., Monteiro, R., Mummery, C., Fisman, G., Cogen, A. and Evans, S.** (2006). Isl1Cre reveals a common Bmp pathway in heart and limb development. *Development* **133**, 1575-1585.
**Yelbuz, T. M., Waldo, K. L., Kumiski, D. H., Stadt, H. A., Wolfe, R. R., Leatherbury, L. and Kirby, M. L.** (2002). Shortened outflow tract leads to altered cardiac looping after neural crest ablation. *Circulation* **106**, 504-510.
**Zhang, X. M., Ramalho-Santos, M. and McMahon, A. P.** (2001). Smoothened mutants reveal redundant roles for Shh and Ihh signaling including regulation of L/R symmetry by the mouse node. *Cell* **106**, 781-792.
**Zucker, R. M., Hunter, E. S., 3rd and Rogers, J. M.** (1999). Apoptosis and morphology in mouse embryos by confocal laser scanning microscopy. *Methods* **18**, 473-480.